Taper-integrated multimode-interference based crossings for silicon wire waveguides

Chia-Hsiang Chiu, and Chyong-Hua Chen
Department of Photonics & Institute of Electro-Optical Engineering,
National Chiao Tung University,1001 Ta Hsueh Road, Hsinchu 30010, Taiwan

ABSTRACT

Novel multimode-interference (MMI)-based crossings integrated with miniaturized tapers are numerically presented for Silicon wire waveguides. These miniature tapers function as field expanders to reduce transition loss between the input/output waveguide and the MMI region and the crosstalk in the crossing section. As a consequence, the lengths of MMI sections reduce to less than twice of the beat length. Using finite different time domain method, we demonstrate that the MMI-based waveguide crossing embedded in the quadratic tapers has the size of 5800x5800 nm^2, the insertion loss of 0.15 dB and the crosstalk of -42 dB at the wavelength of 1550 nm and broad transmission spectrum ranging from 1500 nm to 1600 nm.

Keywords: waveguide crossings, multimode interference based device, silicon wire waveguide, integrated photonics

1. INTRODUCTION

Silicon photonics provides a promising on-chip platform for the ultra large-scale photonic integrated circuits (PICs) because high index-contrast silicon wire waveguides confine the light tightly into submicron scales and the well-established complementary metal-oxide semiconductor (CMOS) based processing can be used to fabricate essential optical passive and active components [1-2]. To achieve highly dense PICs with blocks of cross-grid arrays, waveguide crossings with the properties of compact sizes, low insertion loss and low crosstalk are requisite. Conventional waveguide crossings with normal waveguide intersections possess compact dimensions, but they show significant insertion loss and crosstalk in that the guided modes are diffracted divergently and some energy of incidence is radiated away at intersections as a result of losing lateral confinement there.

To mitigate these phenomena and to enhance waveguide crossing performance, various approaches are investigated in literatures. One is a mode-expander type crossing which is designed to broaden the waveguide core adiabatically with either the parabolic or the elliptical shape to reduce wide-angle components of guided modes and, in consequence, diffraction in the crossing region is suppressed [3-4]. However, these designs either have rather large volume or require more complex fabrication process to realize adequate insertion loss and crosstalk.

In addition, multimode-interference (MMI)-based type crossings [5-6] based on the self-image principle [7] of MMI structures to converge the input beam to the size smaller than that of MMI waveguides at the intersection center have been examined to moderate the diffraction and to obtain low loss at crossings . However, to reform a single self-image at the crossing center, the length of the MMI waveguide is required to be at least twice of the beat length. Moreover, adiabatically optimized tapers with their lengths larger than the beat length are indispensable to diminish the transition loss between MMI sections and the input/output waveguide. As a consequence, dimensions of the crossings are extremely expanded.

Here, we numerically present novel taper-integrated MMI based crossings to achieve the properties of compact size, low insertion loss and low crosstalk. These integrated tapers function as a field expander to convert some power of the input guided mode into higher-order modes confined within the MMI sections. With proper design, these taper-integrated MMI sections act like a waveguide lens and the input field is focused at some position of the MMI waveguide as propagating through the structure. By applying this property, we use these taper-integrated MMI sections to compose waveguide crossings and realize their performances numerically by using three-dimensional finite difference time domain (FDTD) method.

*ray_tkd@msn.com; phone 886-3-5712121-56350; fax 1-886-3-5716631;

Silicon Photonics V, edited by Joel A. Kubby, Graham T. Reed, Proc. of SPIE Vol. 7606, 76061C

2. MMI BASED WAVEGUIDE CROSSING DESIGN

A single-mode ridge waveguide made of Silicon (n=3.45) deposited on a SiO_2 layer (n=1.45) with a width W_g of 500 nm and a height H of 220 nm is designed as the input and the output waveguides. The concerned wavelength is fixed to 1550 nm. The waveguide crossing is composed of two 90° intersecting MMI waveguide structures sandwiched between four identical taper sections, as schematically shown in Fig. 1. The width of the MMI waveguide (W_m) is designed to be 1200 nm to support three TE-like modes (i.e. TE_{00}, TE_{01} and TE_{02} modes) and its length is L_m. The width of the taper varies from W_g to W_m with its length L_t. These components have the same height as the input/output waveguide, i.e. 220 nm. A semi-vectorial three-dimensional (3D) FDTD method is used to calculate the performance of this device with the fundamental TE-like mode of the input waveguide ($TE_{00,in}$ mode) as the incident wave.

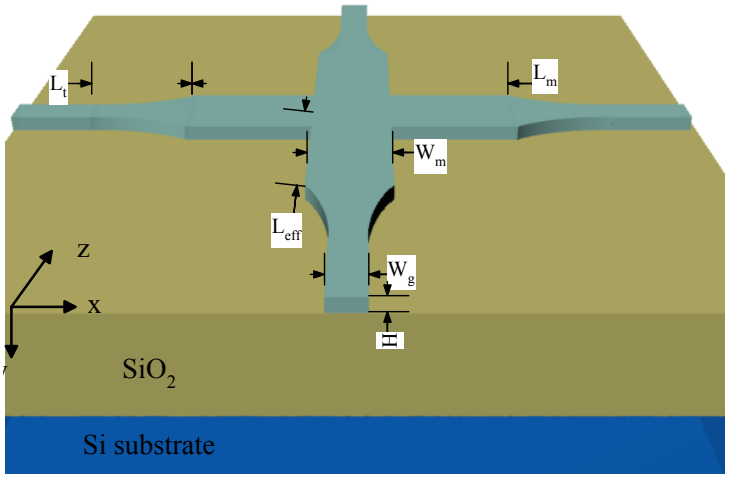

Fig. 1 Schematic structure of the proposed waveguide crossing

2.1 Self-image formation by guided mode propagation analysis

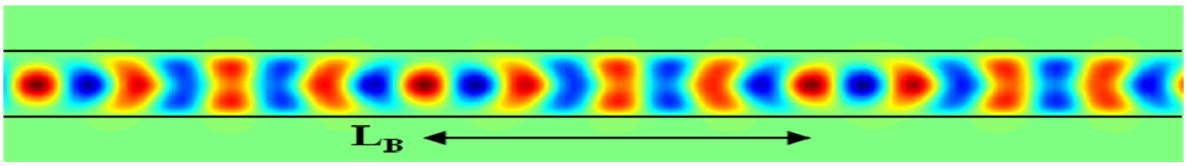

Fig. 2 Field distribution propagated along the MMI waveguide with C_0=0.94 and C_2=0.34

When an arbitrary field in the input waveguide propagates into the MMI section, the field profile $E_{in}(x,y)$ at the interface of the input waveguide and the MMI section can be decomposed into the modal field distributions $E_i(x,y)$ of even eigenmodes of the MMI waveguides because of structure symmetry and given by

$$E_{in}(x,y)=\sum_{i=0}^{N} C_i E_i(x,y) \tag{1}$$

where C_i is the modal coefficient of the mode field distribution $E_i(x,y)$, i=0..N, and calculated by using overlap integral

$$C_i=\frac{\iint E_{in}(x,y)E_i(x,y)dxdy}{\iint E_i(x,y)E_i(x,y)dxdy} \tag{2}$$

In our design, only two lowest-order even guided modes are excited (i.e., TE_{00} and TE_{02} modes) and the field distribution at some distance z of the MMI section can be written as superposition of field distributions of these two guided modes.

$$E_{in}(x,y,z)=C_0E_0(x,y)e^{-j\beta_0 z}+C_2E_2(x,y)e^{-j\beta_2 z} \tag{3}$$

where β_i is the propagation constant of the mode field $E_i(x,y)$, i=0 and 2.

As been seen in Eq. (3), $E_{in}(x,y)$ inside the MMI waveguide can be reproduced at certain length L as the phase changes of the TE_{00} and TE_{02} modes at L differs by $2m\pi$, where m is an integer. Figure 2 shows the calculated intensity distribution inside the designed MMI section with C_0=0.94 and C_2=0.34. Due to mode interferences, the single self-image along the propagation direction of the MMI waveguide is observed periodically with periodicity of the beat length (L_B) of these two modes defined as

$$L_B = \frac{2\pi}{(\beta_0 - \beta_2)} \tag{4}$$

The effective indices of the TE_{00} and TE_{02} modes at the wavelength of 1550 nm are 2.7299 ($n_{eff,0}$) and 2.0476 ($n_{eff,2}$), respectively, calculated by finite element method. The corresponding beat length L_B of these two modes is equal to 2271 nm.

2.2 Effect of the taper length

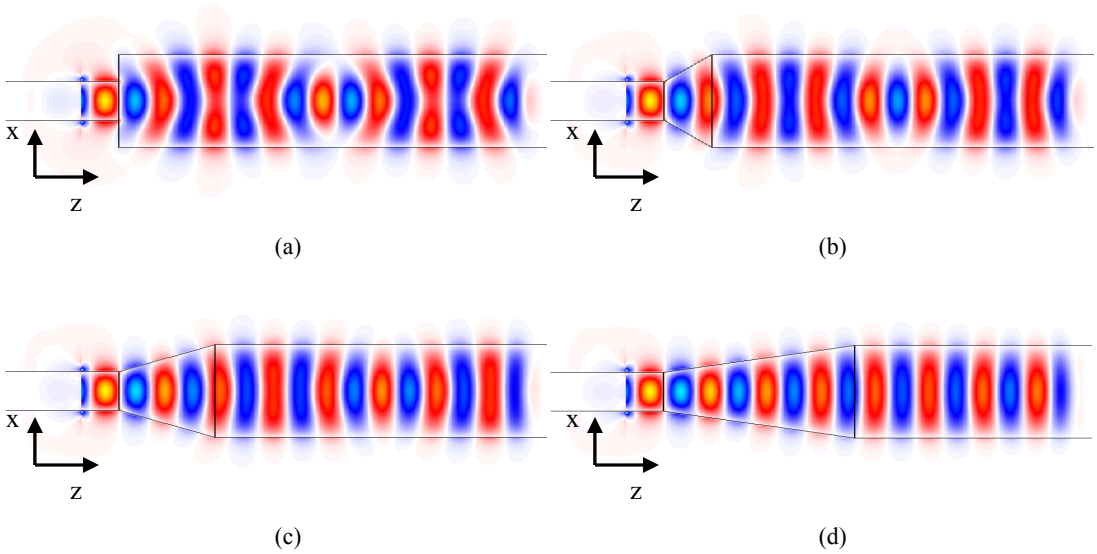

Fig.3 Evolution of the input guided mode propagation through the taper with its length of (a) 0, (b) 500, (c) 1000 and (d) 2000 nm and the MMI section

Conventionally, insertion of a tapered waveguide in between the input and the MMI waveguides is an essential approach to diminish the transition loss between these two dissimilar waveguides. Figure 3 illustrates the simulated propagation behaviors of the fundamental mode of the input waveguide ($TE_{00,in}$ mode) in the linear tapers with different values of L_t sandwiched by the input waveguide and the designed MMI section. We see that the $TE_{00,in}$ mode diverges first and then converges at some distance L_{eff} of the MMI section where the smallest beam waist is observed. Here, we define L_{eff} as the effective beat length of this MMI section. Without inclusion of a taper (as shown in Fig. 3 (a)), the field along the MMI section diffracts dramatically first and then converges at $L_{eff}=L_B$. As the taper length increases, the beam divergence of the field at the end of the taper decreases because most power of the $TE_{00,in}$ mode is converted into the TE_{00} mode.

In addition, we notice that the effective beat length (L_{eff}) and the beam waist calculated by e^{-1} width of the optical field at L_{eff} of the MMI section are varied with the taper length L_t. Variations of the effective beat length L_{eff} and the total length ($L_{eff}+L_t$) with the taper length L_t are shown in Fig. 4 (a). As the taper length L_t increases, the effective beat length L_{eff} decreases. On the other hand, the total length increases monotonically with the taper length L_t. It manifests the required length to obtain the smallest beam waist in the structure constructed by this MMI section integrated with a linear taper is larger than the beat length L_B.

Figure 4(b) depicts the beam waist at L_{eff} of the MMI section as a function of the taper length L_t. The beam waist increases with the increases of the taper length L_t as L_t<1600nm and approximately is unvaried as L_t>1600 nm. As L_t=0, the beam waist is roughly equal to 550 nm, much wider than that of the $TE_{00,in}$ mode (~400 nm). This mismatch implies

that some power of the $TE_{00,in}$ mode is lost due to finite number of guided modes confined within the MMI section. The calculated coupling efficiencies from the $TE_{00,in}$ to the TE_{00} and TE_{02} modes are 82.49 % and 13.08%, respectively. The total coupling efficiency from the input waveguide to the MMI region is 95.57%, indicating the transition loss of 0.20 dB in the case of L_t=0. As L_t>1600 nm, the beam waist roughly equals to 850 nm, slightly smaller than that of the TE_{00} mode (~930 nm) because most power of the $TE_{00,in}$ mode transfers into the TE_{00} mode.

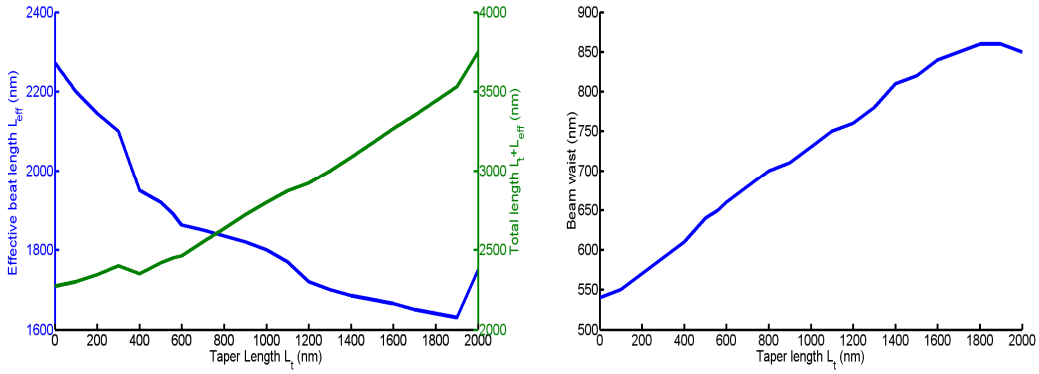

(a) (b)

Fig.4 (a) Effective beat length L_{eff} (blue line) and the total length $L_{eff}+L_t$ (green line), and (b) beam waist at L_{eff} of the MMI section as a function of taper length L_t

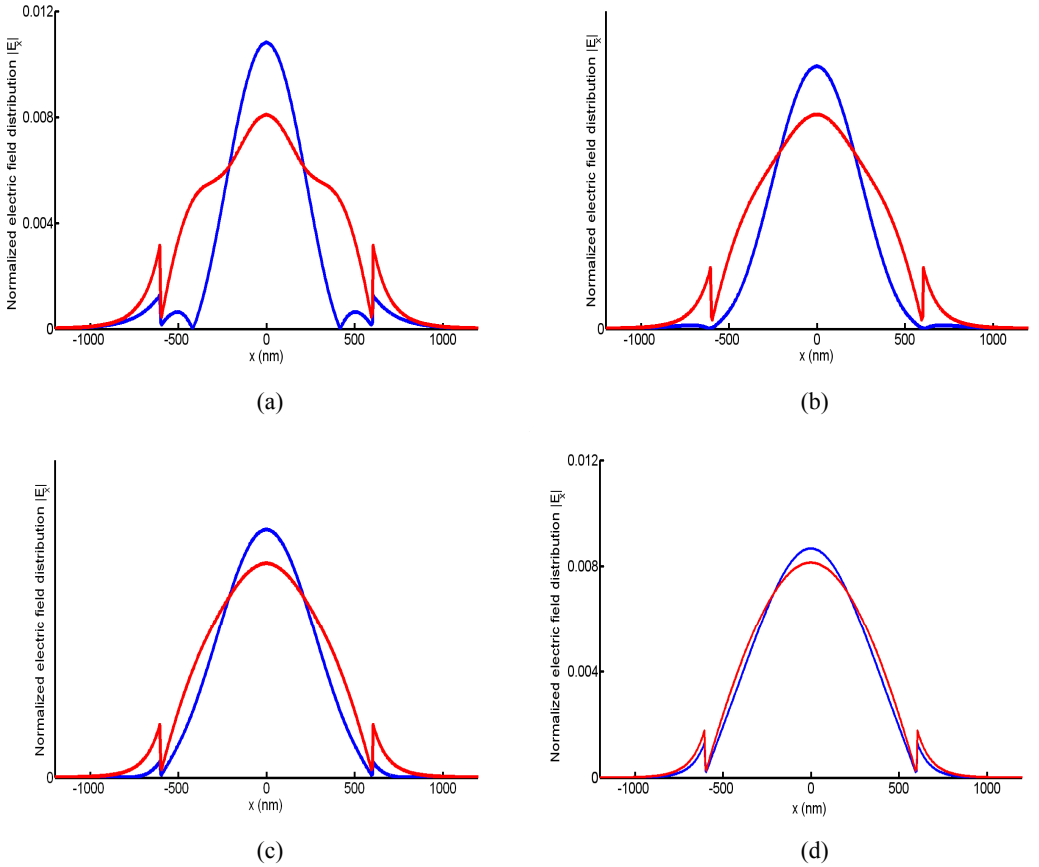

(a) (b)

(c) (d)

Fig.5 Variations of field distributions normalized by the power of the fields in the x direction at L_{eff}-W_m/2 (red curves) and L_{eff} (blue curves) of the MMI waveguide for the taper length L_t of (a) 0, (b) 560, (c) 1000 and (d) 2000 nm

We find that the change of the taper length results in different transferred power ratio of the TE_{00} to the TE_{02} mode. Based on Eq. (3), the field profile along the MMI section can be determined by the amplitude ratio of C_0 to C_2 defined as η. Figure 5 displays the electric field distributions in the x direction at L_{eff}-$W_m/2$ and L_{eff} of the MMI section as L_t=0, 560, 1000 and 2000 nm with the corresponding η= 1.95, 3.66, 5.56 and 14.44. As been seen in Fig. 5 (a), the electric field spreads over the guided area at L_{eff}-$W_m/2$ of the MMI section and a focusing beam with ripples inside the guided region is discovered at L_{eff} of the MMI section in the case of L_t =0. At L_{eff}-$W_m/2$ of the MMI section, the field inside the guided region is concentrated and the field distribution gradually becomes that of the TE_{00} mode as L_t increases. At L_{eff} of the MMI section, the field inside the guided region gradually expands as L_t increases. Furthermore, ripples inside the guided region disappear and the intensity of the field at the interface of the guided region and the air increases with the increase of L_t as L_t>560 nm. Field distributions at L_{eff}-$W_m/2$ and L_{eff} of the MMI section are approximately the same as L_t becomes larger than 1000 nm because the field profile is dominated by the TE_{00} mode. In the case of L_t=560 nm, the field distribution is like a focusing Gaussian beam with beam waist=328 nm at L_{eff} of the MMI section.

We use the aforementioned taper-integrated MMI section with the lengths of the taper and MMI section of L_t and L_m=2L_{eff} to construct four-fold symmetric waveguide crossings. Figure 6 shows the input guided $TE_{00,in}$ mode propagates through the implemented waveguide crossings with L_t=0, 560, 1000 and 2000 nm. In the case of L_t=0 as shown in Fig. 6(a), we discover light is diffracted dramatically at the crossing section and significant scattering radiates into the orthogonal MMI sections due to no lateral guiding mechanism though a focusing beam at the center of the crossing is observed. In the case of L_t=560 nm, we see a narrowing beam at the center of the crossing and nearly identical wave fronts with reversal sign of phases at the front and back of the crossing. Figure 6(c) and (d) show wave front expands through the crossing without tremendous irregular scattering and crosstalk because the dominant TE_{00} mode has a narrow angular spectrum.

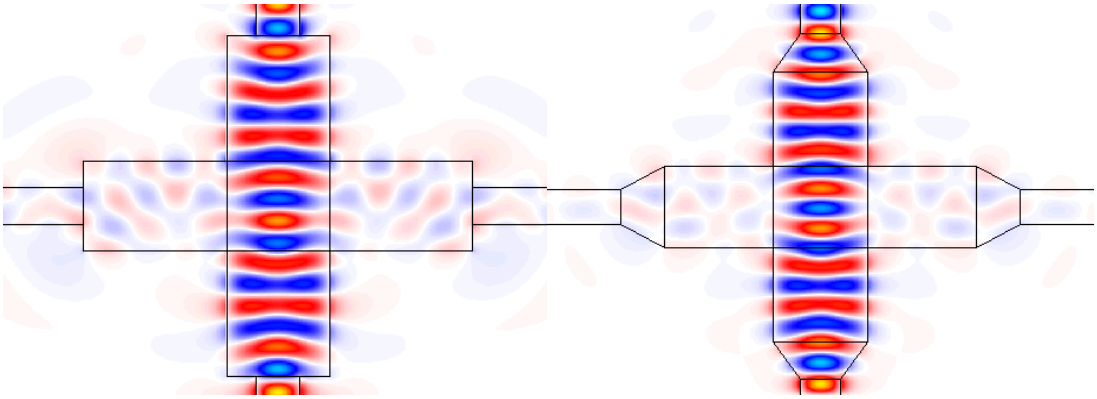

(a) (b)

(c) (d)

Fig.6 FDTD simulations of the input guided mode propagation through MMI based waveguide crossings sandwiched by four identical linear tapers with (a) L_t=0 and L_m=4543.4 nm, (b) L_t=560 nm and L_m=3778.5 nm, (c) L_t=1000 nm and L_m=3600 nm and (d) L_t=2000 nm and L_m=3450.4 nm.

Table 1 Properties of MMI waveguide crossings integrated with linear tapers at the wavelength of 1550 nm

L_t (nm)	η	L_{eff} (nm)	Total length of the crossing L_m+2L_t (nm)	Insertion loss (dB)	Crosstalk (dB)
0	1.95	2271.7	4543.4	0.78	-23.19
560	3.66	1889.3	4898.5	0.24	-45.39
1000	5.56	1800.0	5600.0	0.25	-48.12
2000	14.45	1725.2	7450.4	0.43	-50.63

Table 1 lists the parameters and performance of these four taper-integrated MMI crossing structures with different taper lengths discussed here. As η increases, dimension of the crossing increases but crosstalk decreases. We obtain the smallest insertion loss and rather negligible crosstalk in the case of L_t=560 nm. In the case of L_t=0, the loss caused by intersection structure is roughly equal to 0.58 dB. In the cases of η=5.56 and 14.45, the increase of the insertion loss results from mode mismatches between the guided modes of the MMI section and already diverged beams at the back of the crossing. Compared with the MMI waveguide crossing in the absence of the tapers (i.e. the case of L_t=0), taper-integrated waveguide crossings demonstrate smaller insertion loss and less crosstalk.

In summary, introduction of a miniaturized taper waveguide can not only mitigate the transition loss between the input/output and the MMI waveguides, but also reduce the insertion loss and the crosstalk of the waveguide crossing. With a specificη, optimized performance of the designed waveguide crossing can be carried out.

2.3 Effect of the taper profiles

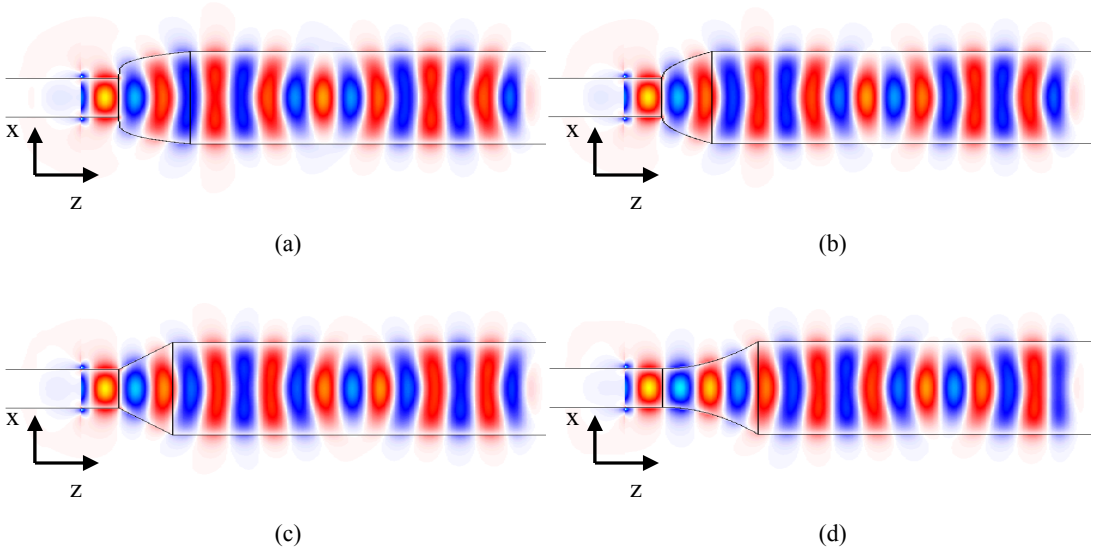

Fig.7 Evolution of the input guided mode propagation through different taper profiles with n= (a) 0.25, (b) 0.5, (c) 1 and (d) 2 and the MMI section

In previous discussion, we realized a focusing beam at the center of the crossing and the smallest insertion loss as the amplitude ratio of two lowest-order guided modes C_0 to C_2 (η) =3.66 inside the MMI section. Here, we investigate the performance of the proposed waveguide crossings with different transverse taper profiles. The studied taper profiles expand in width with an initial value of 500 nm to the final value of 1200 nm and are given by

Table 2 Performance of waveguide crossings with different taper profiles at the wavelength of 1550 nm

n	L_t (nm)	L_{eff} (nm)	Total length of the crossing L_m+2L_t (nm)	Insertion loss (dB)	Crosstalk (dB)
0.25	750	1400.0	4300.0	0.37	-39.83
0.5	530	1735.0	4530.0	0.33	-42.85
1	560	1889.3	4898.5	0.24	-45.39
2	1000	1900.0	5800.0	0.15	-42.34

$$W_t(z) = 500 + (1200 - 500)\left(\frac{z}{L_t}\right)^n \quad (5)$$

where $W_t(z)$ is the taper width in nm and L_t is the taper length.

To realize η=3.66, L_t are chosen to be 750, 530, 560 and 1000 nm, respectively, corresponding to the cases of n=0.25, 0.5, 1 and 2. Figure 7 exhibits the simulated propagation behaviors of the $TE_{00,in}$ mode through these taper-integrated MMI sections. We observe the $TE_{00,in}$ mode diverges along this transverse taper and then converges at L_{eff} of the MMI section with the same beam waist due to the fixed value of η. The corresponding L_{eff} of 1400, 1735, 1889 and 1900 nm and transition losses of 0.17, 0.12, 0.09 and 0.02 dB are calculated with respect to the cases of n=0.25, 0.5, 1 and 2, respectively.

Table 2 summarizes the performance of simulated MMI crossings at the wavelength of 1550 nm using different L_t values and corresponding optimized L_m values for the cases of n=0.25, 0.5, 1 and 2. The dimension of the crossing increases with the increase of n and the total length of the crossing is less than twice of the beat length in the cases of n=0.25 and 0.5. In the cases of small n, more insertion loss is realized due to steep transverse variation in tapers. In addition, the crosstalks in these designs are imperceptible, roughly -40dB.

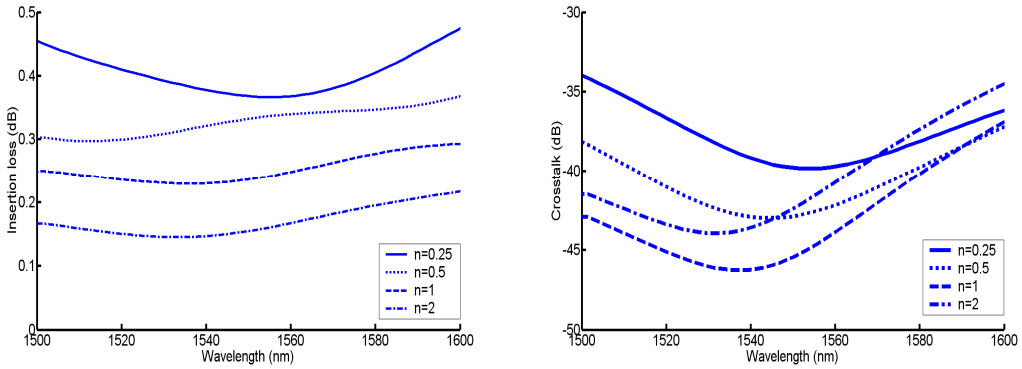

(a) (b)

Fig.8 (a) Simulated insertion loss spectra and (b) calculated crosstalk spectra of the designed MMI waveguide crossings for n=0.25 (solid curves), 0.5 (dotted curves), 1 (dashed curves) and 2 (dashed-dotted curves)

Insertion losses and crosstalks of the aforementioned waveguide crossing designs for n=0.25, 0.5, 1 and 2 as a function of wavelength are shown in Fig. 8 (a) and (b), respectively. The insertion loss decreases with the increase of n in the spectrum ranging from 1500 nm to 1600 nm. In the case of n=2, the insertion loss is averagely 0.18 dB and the crosstalk is less than -40 dB. These results indicate these crossings exhibit broad transmission spectra around 1550 nm.

3. CONCLUSION

We demonstrate a new design approach to achieve compact crossings by use of a taper-integrated MMI waveguide structure. This taper converts some power of the input guided wave into higher-order modes of the MMI waveguide not

only to diminish the transition loss between the input/output waveguide and the MMI region but also to reduce the required length to produce the smallest beam waist inside the MMI region. By investigating the effects of taper lengths and profiles in the proposed waveguide crossings, we find the performance of a MMI waveguide crossing is determined by the amplitude ratio of two lowest-order guided modes supported by the MMI section. Simulation results show that a MMI waveguide crossing integrated with quadratic tapers has the size of 5800x5800 nm^2, the insertion loss of 0.15 dB, the crosstalk of -42 dB at 1550 nm and broad wavelength transmission spectrum. Better performance can be achieved by optimizing the taper design.

REFERENCES

[1] Jalali, B., "Can silicon change photonics?," Physica Status Solidi a-Applications and Materials Science **205**, 213-224 (2008).

[2] Lipson, M., "Guiding, modulating, and emitting light on silicon - challenges and opportunities," Journal of Lightwave Technology **23**, 4222-4238 (2005).

[3] Fukazawa, T, Hirano, T., Ohno, F., and Baba, T., "Low loss intersection of Si photonic wire waveguides," Japanese Journal of Applied Physics Part 1-Regular Papers Short Notes & Review Papers **43**, 646-647 (2004).

[4] Bogaerts, W., Dumon, P., Van Thourhout, D., and Baets, R., "Low-loss, low-cross-talk crossings for silicon-on-insulator nanophotonic waveguides," Optics Letters 32, 2801-2803 (2007).

[5] Liu, H. L., Tam, H., Wai, P. K. A., and Pun, E. "Low-loss waveguide crossing using a multimode interference structure," Optics Communications 241, 99-104 (2004).

[6] Chen, H. and Poon, A. W., "Low-loss multimode-interference-based crossings for silicon wire waveguides," IEEE Photonics Technology Letters **18**, 2260-2262 (2006).

[7] Soldano, L. B. and Pennings, E. C. M., " Optical multi-mode interference devices based on self-imaging: principles and applications," Journal of Lightwave Technology **13**, 615-627 (1995).